Topic editor

The manuscript presents a novel effort to generate the first global 500m resolution mean leaf inclination angle (MLA) product, along with associated leaf projection function data. This work contributes significantly to the field by addressing gaps in phenological and vegetation structure parameters critical for land surface models and remote sensing applications. Both reviewers acknowledge the scientific novelty of the study, the rigorous methodological approach, and its potential to improve vegetation modeling and remote sensing parameter inversion.

However, the reviewers raised significant concerns about methodological robustness, particularly regarding upscaling LIA field measurements, handling coarse-resolution data, and the selection of predictive features. Reviewer 1 emphasized the need for better clarification and testing of the upscaling processes and questioned the reliance on MODIS-based data for capturing LIA signals. Reviewer 2 highlighted the importance of incorporating additional remote sensing parameters and addressing uncertainties in the data sources. Furthermore, both reviewers pointed out the need to better validate the product and address apparent biases, such as overestimation in specific cases.

While the study provides a strong foundation, addressing these concerns through more rigorous uncertainty analysis, methodological refinement, and clearer discussion of data limitations will be necessary for the next revision. The potential to refine global vegetation models and ecological understanding underscores the importance of this work, warranting reconsideration after major revisions.

We thank the topic editor for the recognition and professional processing. We fully understand the concerns raised by the reviewers and have carefully addressed these issues in this revision round.

Some major revisions were made in the revised version:

(1) The concerns regarding the upscaling approach and modeling inputs have been explained.
(2) The uncertainties in the data sources and upscaling process have been analyzed (section 4.4).
(3) The necessity of introducing additional remote sensing parameters to MLA mapping has been analyzed.

(4) The validity of using G(0) validation to evaluate MLA indirectly has been demonstrated (section 4.1).

(5) A regional analysis of variable importance has been conducted (section 4.2).

(6) Some other revisions for the manuscript and supplement material have been made.

Please see the itemized responses below.

Anonymous Referee #2

I agree that Leaf Inclination Angle (LIA) is indeed a critical parameter for global land surface models, such as Dynamic Global Vegetation Models (DGVM). However, after reviewing the authors' responses, I find that most of my original comments remain unaddressed or insufficiently tested. Although this is the first global LIA product, as the authors claim, potential issues in both the upscaling approach and modeling inputs raise substantial concerns about its reliability.

We thank the referee for the recognition and thorough comments that helped us improve the manuscript. We fully understand the referee's concerns regarding upscaling approach and modeling inputs and have provided detailed explanations below. We think much of the misunderstanding is caused by the different requirements for canopy traits between the remote sensing and plant physiology communities.

Regarding my second comment on "Upscaling LIA Field Measurements," the authors mentioned that "in field measurements, the entire canopy LIA is calculated as the average of all measured leaf LIAs weighted by leaf area." I question why leaf area, rather than leaf number, is used for this weighting. Given the highly variable nature of LIA within a canopy and across species and ecosystems (as noted in my first comment), upscaling LIA measurements from site level to 30m, and subsequently to 500m scales, is a crucial initial step. Yet, it remains unclear how the authors executed these steps or assessed the associated uncertainties. Using leaf area rather than leaf number for weighting raises concerns about the representativeness of the measurements.

This is an excellent point. In this study, two different weighting methods were used: (1) from leaf to canopy scale, leaf number was used; and (2) from 30 m to 500 m, leaf area was used. From leaf to canopy scale, the entire canopy LIA is commonly calculated as the average of all measured leaf LIAs weighted by leaf area in the remote sensing community (Zou et al., 2014; De Wit, 1965; Yan et al., 2021). For example, Yan et al. (2021) stated that *the final leaf angle distribution is obtained by weighting the **relative areas** with different leaf inclination angles*. Leaves with larger areas contribute more to photosynthesis and have higher weights. In practice, because of the difficulty in leaf area measurement, especially for a large number of leaves, the variability of leaf areas within a canopy is often ignored and the areas of all leaves are assumed similar. In this case, the canopy LIA can be simplified as the average LIA weighted by leaf number (Ryu et al., 2010; Pisek et al., 2011; Chianucci et al., 2018). Therefore, in this study, the canopy LIA measurements were also obtained by weighting leaf LIA with leaf number.

The obtained canopy LIA measurement was used to represent the LIA at the 30 m pixel level considering the representativeness. The LIA upscaling from 30 m to 500 m was weighted by the 30 m leaf area index (using EVI2 as a proxy). Leaf area index (LAI) is defined as the half of green leaf area on the unit of ground area and is similar to leaf number/density to some extent (Fang et al., 2019). High leaf number typically means high LAI. For a 30 m pixel with a higher LAI, its weight/contribution to the 500 m scale LIA is also higher (Fig. R1).

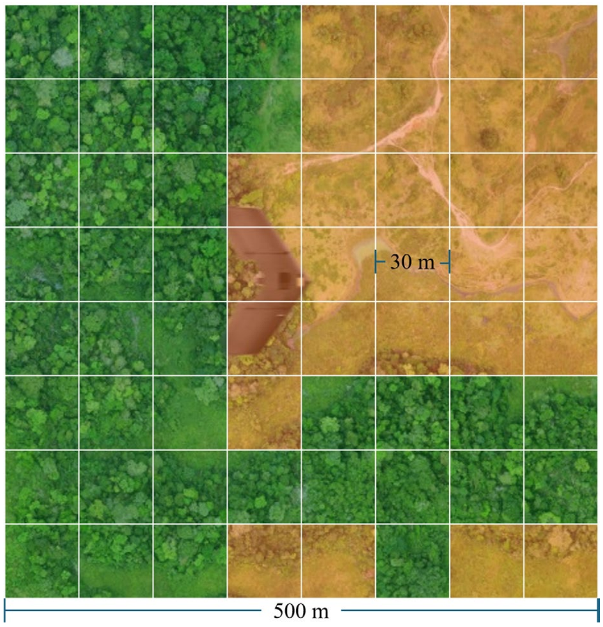

Fig. R1. Schematic of LIA upscaling from 30 m to 500 m. The green and yellow colors denote high and low leaf area index, respectively.

When one plant function type (PFT) within a 500 m pixel has no LIA measurement, the LIA of the PFT was assigned with the value of its nearest neighbor within 100 km with the same PFT. This upscaling practice has been used to map global leaf traits (specific leaf area, leaf dry matter content, leaf nitrogen and phosphorus content per dry mass, and leaf nitrogen/phosphorus ratio) at 500 m spatial resolution (Moreno-Martínez et al., 2018).

For my third comment on “Coarse Resolution and Low-Signal Inputs in the Model,” I feel the authors' response is also lacking. The BRDF product primarily normalizes surface reflectance by mitigating inconsistencies arising from varying sun and sensor angles. With the current 500m resolution, the fine-scale signal of LIA is vulnerable to interference from surface structures, such as canopy heterogeneity, surface roughness, height, clustering, branch structures, and terrain. I am skeptical that MODIS's passive optical sensor can capture LIA signals effectively (Such signals may be better detected by radar or lidar data). Additionally, the claim that "Under suitable climate conditions, horizontal leaves can make better usage of precipitation and increase the photosynthesis rate" is problematic. Water use efficiency is unlikely to be closely related to leaf angles. Currently, NDVI is tested as the primary indicator for LIA, yet NDVI primarily reflects chlorophyll content, which is largely decoupled from information on leaf inclination angle.

Our study has used the BRDF model parameters product (MCD43A1 C6.1, https://lpdaac.usgs.gov/products/mcd43a1v006/) as the predictive variables. MCD43A1 provides three model weighting parameters for different kernels (isotropic, volumetric, and geometric), which can be employed to compute the directional reflectance (Schaaf et al., 2002). We suspect that the referee has mistaken the BRDF product as the Nadir Bidirectional Reflectance Distribution Function (BRDF)-Adjusted Reflectance (NBAR) (MCD43A4, https://lpdaac.usgs.gov/products/mcd43a4v006/), which is derived from MCD43A1 but is normalized to a unified nadir viewing geometry. It is true that the nadir reflectance is difficult to retrieve LIA, as demonstrated by a previous study (Bayat et al., 2018). Nonetheless, the directional reflectance variation is sensitive to LIA (Fig. R2) and has been used to derive LIA from many passive optical sensors (Jacquemoud et al., 2009; Goel and Thompson, 1984; Jacquemoud et al., 1994; Li et al., 2023).

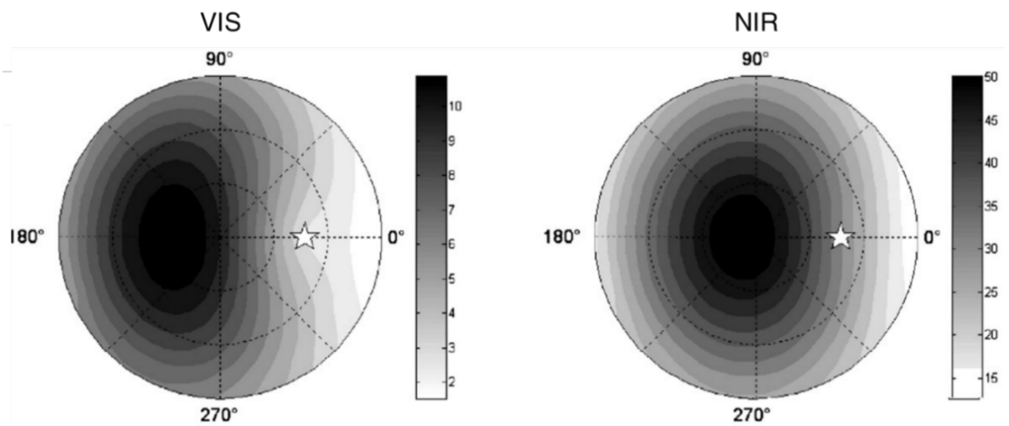

Fig. R2. Contribution of LIA (%) to the top-of-canopy directional reflectance (excerpted from Jacquemoud et al. (2009)). The solar zenith angle (31.6°) is indicated by a star.

At 500 m, the multi-angle reflectance information is related to the average canopy LIA at the same scale. The terrain variables were introduced in the LIA prediction, which partly mitigates the interference from surface structures. As illustrated in Figs. 6 and 7, the BRDF parameters at 500 m scale are sensitive to LIA, further indicating the validity of this practice. In addition, detecting LIA with radar remains in the simulation stage (Lang and Saleh, 1985) and no practical studies have been reported. Point cloud LiDAR has been used to measure LIA accurately but is limited to a local scale due to the limitation of the sensor platform (Zheng and Moskal, 2012; Bailey and Mahaffee, 2017; Itakura and Hosoi, 2019). Currently, no study has used spaceborne LiDAR to estimate LIA.

We agree that the original claim "*Under suitable climate conditions, horizontal leaves can make better usage of precipitation and increase the photosynthesis rate*" is not solid. Under suitable climate conditions (radiation, precipitation, and temperature), the elements required for photosynthesis are satisfied, and horizontal leaves are formed to absorb more radiation and increase the photosynthesis rate (Van Zanten et al., 2010; King, 1997). We have rephrased it as (line 379)

> "*Under suitable climate conditions (radiation, precipitation, and temperature), horizontal leaves are formed to absorb more radiation and increase the photosynthesis rate (Van Zanten et al., 2010; King, 1997)*".

We agree NDVI is related to chlorophyll content, but only when LAI is high (LAI >= 4) (Fig. R3). When LAI < 4, NDVI is strongly coupled with LIA. Globally, the global mean LAI is ~1.20 and high LAI (>=4) only occupies a tiny fraction (Fang et al., 2021). NDVI is frequently used to retrieve canopy structural parameters, such as leaf area index, and fractional vegetation cover (Carlson and Ripley, 1997; Carlson et al., 1994; Wang et al., 2005), but was rarely used for the chlorophyll content, which is more closely related to various chlorophyll indexes formulated by green, red, NIR, and red-edge bands (Dong et al., 2019; Haboudane et al., 2002; Gitelson et al., 2003; Wu et al., 2008). In this study, NDVI is an important contributor to the LIA prediction (Figs. 6 and 7). The correlation between LIA and NDVI has been reported in many simulation and field studies (Fig. R3) (Zou and Mõttus, 2015; Liu et al., 2012; Dong et al., 2019; Jacquemoud et al., 1994) and has been explained in section 4.2. Higher LIA means lower radiation interception, more NIR downward radiation, and lower NIR reflectance (Liu et al., 2012). This results in a negative correlation between LIA and NDVI. In addition, besides NDVI, we have used many other important indicators (including climate, BRDF, terrain) that are related to LIA to predict MLA.

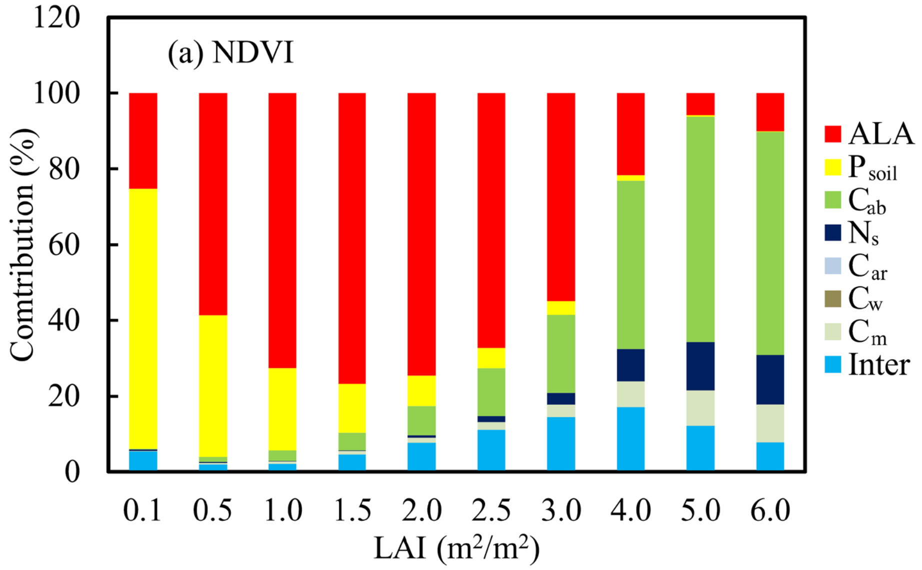

Fig. R3. Contribution of various leaf and canopy properties to the variability of NDVI (excerpted from Dong et al. (2019)). ALA (average leaf angle) is the LIA in this study.

Referee #3

Leaf inclination angle (LIA) is a crucial feature influencing the physiological activities of vegetation leaves and an important parameter for modeling vegetation radiative transfer. However, the global LIA map is very difficult to generate. Based on valuable and incomplete field measurements and other data sources, this paper generates the first global 500m resolution mean leaf inclination angle (MLA) and the lowest point leaf projection function G(0) products by employing nearest-neighbor interpolation, random forest regression, and other algorithms. It also presents the distribution characteristics of global LIA in different vegetation functional types (PFTs) and regions, filling the gaps in related fields. Overall, the study shows highly novelty, with scientific research methodology and detailed data analysis. The results possess certain application potentials, particularly in remote sensing parameter inversion and land surface model application. Nevertheless, there are still improvements to this manuscript. My detailed comments are as follows:

We thank the referee for the recognition and insightful comments which significantly improved the manuscript. We fully understand the referee's concerns and have provided detailed explanations and revisions below.

Major Comments

1. Three different sources of measurements of LIA were used to generate more training samples for machine learning (ML). However, these three types of samples have varying confidence and spatial coverage, e.g., TRY data is mainly in South American. I think this will have an impact on ML training with unequal weights. More detailed analysis and discussion about the uncertainties and representativeness of samples are needed.

We agree these three types of samples (from TRY, literature, and manual extraction) have varying confidence. We think the predicted LIA is robust to these varying issues because part of the samples and features are randomly selected in the training process and the random forest algorithm ensembles the predications from multiple decision trees (Svetnik et al., 2003). We have manually inspected all field LIA data and made sure that they are the canopy LIA and field measurements are typically characterized by high confidence.

The LIA measurements in South America are mainly from palms (line 90), while the LIA measurements of most species are located in the Northern Hemisphere. Subsequently, the spatial expansion was conducted with the TRY species location database, which comprises trait measurements for common species representing a hundreds-of-square-meter area around the location. The dominant species was artificially identified by investigators and thus the spatial representativeness is considered. After spatial expansion, the distribution of samples is more uniform (Figs. 4 and S3), and the following rigorous sample screening considering representativeness further reduces the uncertainty of LIA samples. Therefore, the impact of spatial distribution is minimized.

In response to the referee's comment, we have explained it in the discussion part (lines 406 and 422):

> *Three different sources of LIA measurements were gathered with different sampling schemes and methods. The random forest algorithm is robust to these differences because part of samples and features are randomly selected and the algorithm ensembles the predications from multiple decision trees (Svetnik et al., 2003).*
>
> *Using standard LIA measurement protocols will certainly improve the LIA data consistency.*

2. MLA should be mainly controlled by plant genes and age, so vegetation biome map should be the key and first predictive feature for global MLA mapping. And more RS-based vegetation structure parameters (e.g., FVC, height, LAI, CI…) can be added in the predictive features. I hope this can be considered in the next version of this dataset.

We thank the referee for this point. In fact, the plant function type map (MCD12Q1 C6) was initially used as a predictive variable (Tables 1 and 2), but relatively low importance was found for LIA prediction (ranked 47 out of 76). This may be because the biome information is implicitly included in the spectral features as the former is frequently derived from the latter (Sulla-Menashe et al., 2019). Previous studies have demonstrated that the LIA variation within PFT maybe larger than that between PFTs. This indicate that the biome map is not a good predictor (Prentice et al., 2024). To avoid overfitting, only the most important 40 features were used for LIA prediction.

We thank the referee's point about using the RS-based vegetation structure parameters (e.g., FVC, height, LAI, CI…) in the MLA estimation. Similarly, RS-based vegetation structure parameters (e.g., FVC, height, LAI, CI…) are also closely correlated to spectral and BRDF features. For example, LAI and FVC are typically derived from spectral reflectance (Jia et al., 2015; Yan et al., 2022; Fang et al., 2019), and CI satellite product from BRDF (Wei et al., 2019; Fang, 2021). Previous studies indicate that canopy height is also related to BRDF (Wang et al., 2011; Cui et al., 2019; Wang and Ni-Meister, 2019). In addition, these structural parameters (e.g., FVC, height, LAI, CI…) are related to climate (precipitation, radiation, temperature) and topography parameters (Zhang et al., 2004; Amiri et al., 2009; Iio et al., 2014), which were already considered in the MLA mapping. Moreover, too many predictive variables may cause computation limit. Indeed, as the referee pointed out, these parameters can be considered in the MLA mapping in the future.

3. In line 167, you used EV2 as the weight of the pixel instead of LAI. There is no problem if LAI and EVI2 have a good linear relationship. However, this is not always true, especially for dense forests. The real relationship between LAI and EVI2 can be obtained from global statistics and this relationship can be used in Eq. (1). Or the now available 30m LAI products can be used here instead of EVI2. I know this will result in large revision work, so I hope this can be considered in the next version of this dataset.

Thank the referee for this constructive comment. At the beginning of this work, global 30 m LAI was not available. Currently, global 30 m LAI has a big data size and is unavailable on Google Earth Engine (GEE), whereas EVI2 is easy to calculate on GEE for upscaling of a 500 m pixel.

Following the suggestion, we have attempted to use the real MODIS LAI-EVI2 relationship (Fig. R4) from global statistics to correct the MLA upscaling procedure. 2,000 points for each biome type were randomly sampled and the LAI-EVI2 pairs with good quality per 8 days for these points were extracted.

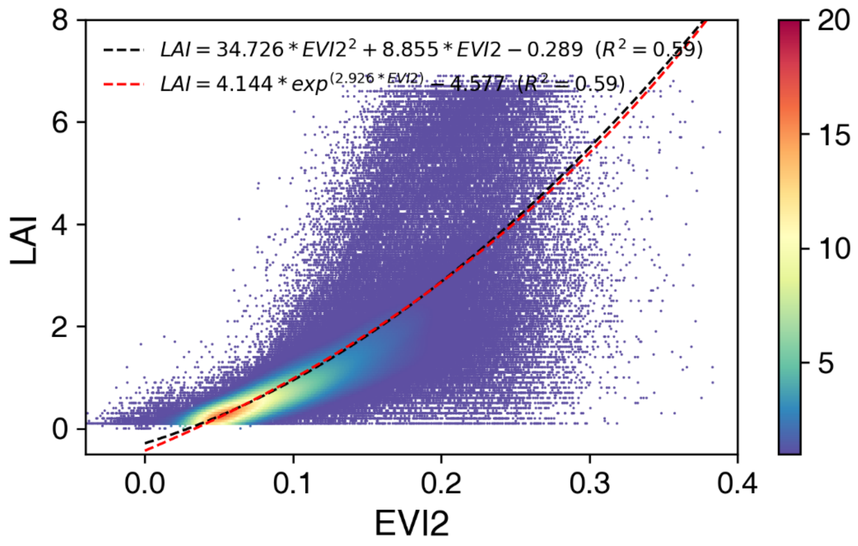

Fig. R4. The nonlinear relationship between MODIS LAI and EVI2.

Subsequently, we have updated the train samples with the fitted nonlinear relationship and compared the samples to the original samples with EVI2. The updated samples show high consistency with the original samples (Fig. R5). This may be related to the rigorous sample screening to keep the homogeneity of a 500 m sample, which reduces the impact of the LAI-EVI2 nonlinear relationship by limiting LAI variations within the 500 m pixel.

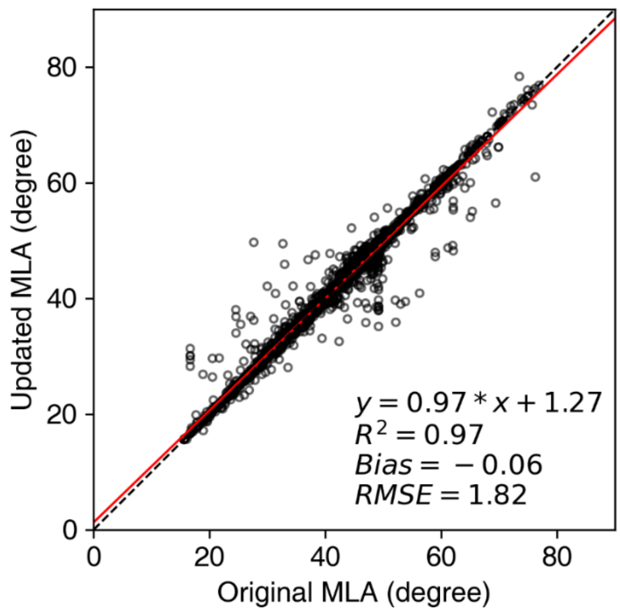

Fig. R5. The comparison between the updated samples using the LAI-EVI2 relationship and original MLA samples using EVI2. The black dashed and red solid lines represent 1:1 and fitted lines.

This issue has been discussed in line 414.

Eq. (1) assumed a linear relationship between LAI and EVI2 in the 500 m upscaling process. Global analysis of MODIS LAI and EVI2 shows a non-linear relationship between the two variables (Fig. S8). This non-linear relationship was also used to upscale MLA, and the derived MLA was found consistent with the original one (Fig. S9) because of the homogeneity of the 500 m pixel after rigorous sample screening (section 2.3.1).

4. As recently found, MCD15A2H has some problems such as internal inconsistency, backup algorithm problem, and spatiotemporal gaps. Better products such as HiQ-LAI and SI (sensor-independent) LAI are also available on GEE and can be used in this study (Maybe in the next version update and this should be discussed in this paper).

We agree with the referee that the MODIS LAI product used for LIA upscaling in the G(0) validation (section 2.4) have some issues such as internal inconsistency, backup algorithm accuracy, and spatiotemporal gaps. Because we used the multi-year average LAI in the G(0) validation, the influence induced by these factors can be partly mitigated.

Following the kind suggestion, we have discussed it in line 361.

> *The MODIS LAI product used for LIA upscaling in the G(0) validation (section 2.4) is known to have issues such as internal inconsistency, backup algorithm accuracy, and spatiotemporal gaps (Kandasamy et al., 2013; Pu et al., 2023; Zhang et al., 2024). In the future, new improved MODIS LAI can be used in the G(0) validation (Pu et al., 2024; Yan et al., 2024).*

5. Fig. 13 shows an obvious overestimation which reduces the credibility of the data. I think it’s not enough just to explain the possible reasons for these results. Instead, ways should be found to eliminate this overestimation. A simple empirical correction may be used here?

Thanks for the referee’s point. We analyzed the potential factors that caused this overestimation, including the limited LIA data volume and reference G(0) quality. But due to the lack of LIA measurement and high-resolution MLA/G(0), it is difficult to find a good solution. Although some empirical adjustment methods may be used, we decide not to do it. We are afraid that it would bring more confusion to readers. Further improvement of the MLA estimation needs a sufficient amount of LIA measurements.

It is noted that the predicted MLA shows good consistency with validation samples (Fig. 12) and the statistics of LIA field measurements (Tables 3 and 4). The results demonstrate the reliability of the predicted MLA.

6. For PFTs with missing LIA measurements, this article assigns the nearest LIA with measured values within 100km to the missing region using the nearest-neighbor interpolation method based on spatial proximity. However, it does not analyze the errors that can be caused by this interpolation method. In addition, is a spatial extent of 100km of interpolation too large for image pixels with a resolution of 500m? It is recommended that the authors cite the relevant literature or perform a quantitative assessment in this regard.

Because of the lack of sufficient LIA measurements for some PFTs in certain locations, the nearest-neighbor LIA assignment has to be employed for the LIA upscaling. The distance setting (100 km) was based on a previous study (Moreno-Martínez et al., 2018) which derived global maps for various leaf traits (specific leaf area, leaf dry matter content, leaf nitrogen and phosphorus content per dry mass, and leaf nitrogen/phosphorus ratio) from a limited number of field measurement, remote sensing, and climate data. Moreno-Martínez et al. (2018) tried different distances and selected a value (100 km) that provided the most stable and reasonable results. We have tried to use a lower distance (50 km), but the final sample number is reduced by more than 50% which makes it difficult to map LIA.

7. Due to the lack of high-resolution MLA data, this paper utilizes the leaf projection G - function derived from MLA for the indirect assessment of MLA. However, it does not elaborate on the scientific validity and reliability of this indirect verification. To what extent can the assessment of the leaf projection function substitute for the assessment of the MLA data itself? It is recommended that the authors provide a more in-depth explanation of this part.

As the referee pointed out, because of the lack of high-resolution MLA data, this paper utilized the nadir leaf projection function for the indirect assessment of MLA. We think this method is valid and reliable mainly because MLA and G(0) are closely related. G(0) is typically calculated from the LIA distribution function based on Nilson's algorithm

(Nilson, 1971). Here, we calculated G(0) from MLA assuming an ellipsoidal LIA distribution (De Wit, 1965). The calculated G(0) is highly consistent with the reference G(0) calculated from the Nilson's algorithm for six theoretical LIA distributions (Fig. R6). The MLA-calculated G(0) shows a monotonic decreasing relationship with MLA (Fig. R7). Indeed, G(0) is more sensitive to MLA at higher MLA values (Fig. R7).

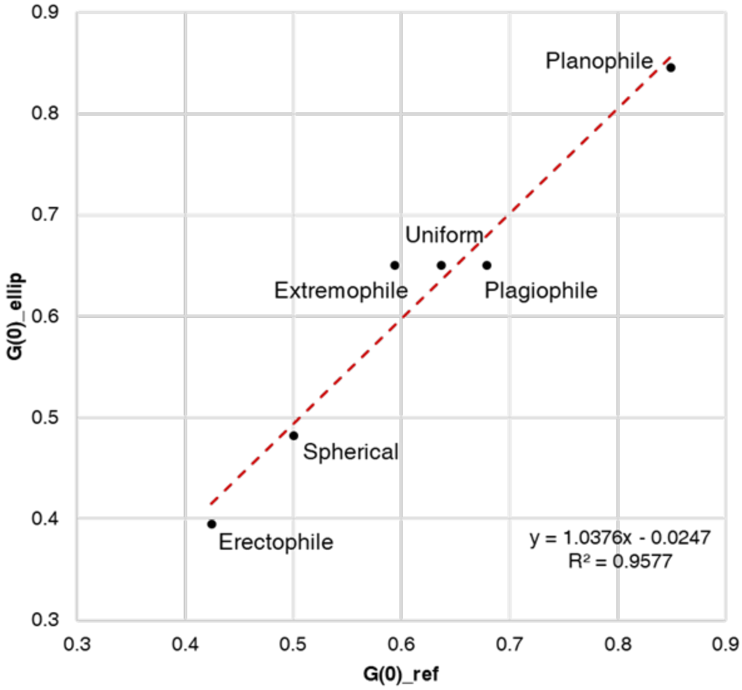

Fig. R6 Comparison of the G(0) calculated from MLA assuming ellipsoidal LIA distribution (G(0)_ellip) and the reference G(0) (G(0)_ref) calculated form the Nilson's algorithm (Nilson, 1971) for six different leaf angle distributions.

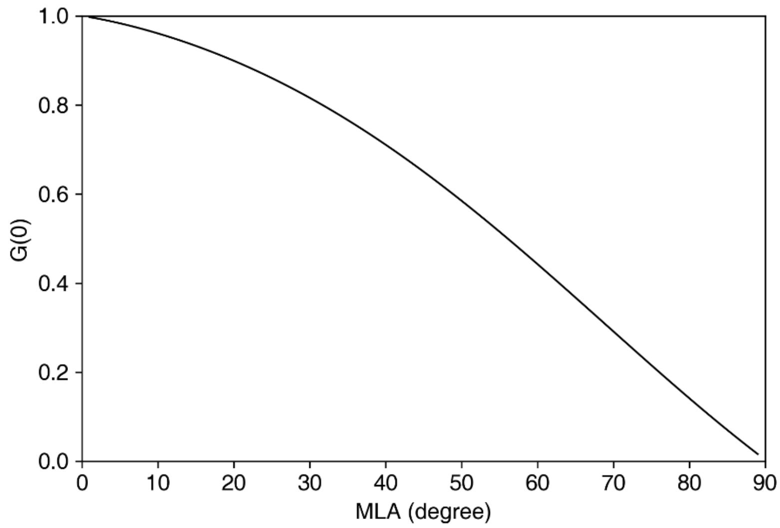

Fig. R7 Variation of G(0) with MLA assuming an ellipsoidal leaf distribution.

In response to the comment, we have explained this in the discussion (line 345).

> *Due to the lack of high-resolution reference MLA, the global MLA was evaluated through a comparison of the MLA-derived G(0) with the high-resolution reference G(0) (Fig. 13). This practice was adopted because both MLA and G(0) are closely related. G(0) is typically calculated from the LIA distribution function based on Nilson's algorithm (Nilson, 1971). We calculated G(0) from MLA assuming an ellipsoidal LIA distribution (De Wit, 1965) and found that the calculated G(0) is highly consistent with the reference G(0) calculated from the Nilson's algorithm for different theoretical LIA distributions (Fig. S5). The MLA-calculated G(0) also shows a monotonic decreasing relationship with MLA (Fig. S6).*

8. Although the paper predicts the 40 most important predictor variables for MLA, it does not evaluate whether the importance of these variables varies among different regions or plant functional types. Given that the outcome of the study is a global map, considering the ecological diversity of different regions, the relationship between MLA and predictor variables such as NDVI, BRDF, and climatic variables may change. It is recommended that the authors conduct a regional analysis of the variable importance to explore these potential differences and discuss their implications for model generalization and ecological interpretation.

We thank the referee's suggestion. As the referee may know, similar global mapping practice have been conducted in many leaf trait mapping studies (Moreno-Martínez et al., 2018; Zhang et al., 2021; Yang et al., 2021; Boonman et al., 2020).

Following the referee's suggestion, we examined the variable importance in different climate zones: the tropical zone (23.5°S-23.5°N), the northern temperate zone (23.5°N-60°N), the northern polar zone (60°N-90°N), and the southern temperate zone (23.5°S-60°S). The 40 most important variables are similar among different regions although minor differences exist (Fig. R8). Among the 40 variables for tropical, northern temperate, northern polar, and southern temperate zones, 32, 35, 30, and 31 of them, respectively, are the same as the 40 global variables (Fig. R8). Climate and spectral variables are significant among all regions, while the BRDF features are the most important in the southern temperate zone. The 40 most important variables in the global MLA prediction account for ~ 80% of total importance among different regions, which is similar to that in the global prediction. We also tested >40 variables and found that too many variables would increase computational complexity without any accuracy improvement due to variable redundancy.

We have discussed it in line 384.

> *This study predicted global MLA with 40 variables (Fig. 6). To explore the regional differences of the variable importance, an analysis was conducted for the tropical (23.5°S-23.5°N), northern temperate (23.5°N-60°N), northern polar (60°N-90°N), and the southern temperate (23.5°S-60°S) zones. The 40 most important variables are similar among different regions although minor differences exist (Fig. S7). Among the 40 variables for tropical, northern temperate, northern polar, and southern temperate zones, 32, 35, 30, and 31 of them, respectively, are the same as the 40 global variables (Fig. S7). Climate and spectral variables are significant among all regions, whereas BRDF features are the most important in the southern temperate zone. The 40 most important variables in the global MLA prediction account for ~ 80% of total importance among different regions, which is similar to that in the global prediction.*

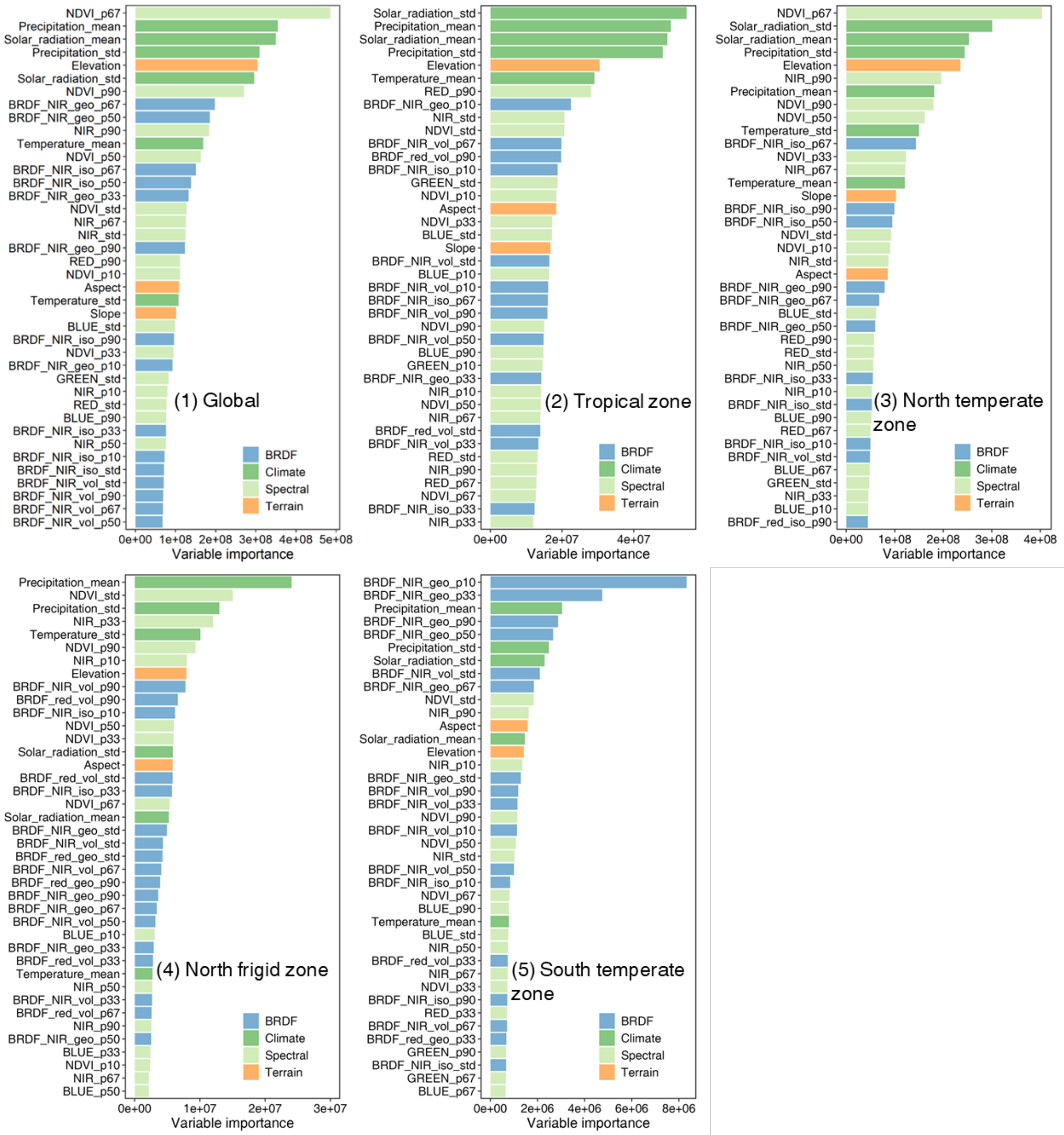

Fig. R8 The variable importance among different climate zones.

Minor Comments

1. In Figure 2, some of the legends overlap one another, resulting in a rather unclear display. It would be advisable to use legends with more distinct contrast. Fig.2b and 2c can be deleted.

We have updated fill and edge colors with more distinct contrast and deleted Fig. 2b and c.

2. Figure 9(a) and Figure 5 are repetitious in terms of illustration form, which appears somewhat redundant. The information of these two figures can be entirely presented

in one figure. It is proposed that one of the two figures be replaced by a geographical map.

Fig. 5 shows the biome distribution of MLA field measurements, while Fig. 9 (a) is the biome distribution of the MLA map. Fig. 5 is difficult to be replaced with a geographical map, because of the lack of locations for several MLA measurements.

3. The description of the verification of the global MLA map from line 196 to line 200 is somewhat muddled. It would be better to directly clarify why G(0) is used for verification.

Thank you for the suggestion. We have revised it (line 195).

The global MLA map was indirectly evaluated using the nadir leaf projection function, because of the lack of high-resolution reference MLA. G(0) is important because it is coherent with the satellite nadir observations. The global G(0) was derived from the MLA and evaluated with high-resolution reference following the upscaling scheme recommended by the Land Product Validation (LPV) Subgroup of the Committee on Earth Observation Satellites (CEOS) (http://lpvs.gsfc.nasa.gov/).

4. There seems to be a problem with the format of Table 3 between lines 239 and 240.

Thank you for your reminding. We have checked it and found this problem is caused by page crossing. The format of Table 3 doesn't have any problems.

5. In line 248, only the significant influence of altitude on MLA prediction is mentioned.

We have revised it.

In addition, elevation, slope, and aspect significantly impact on the MLA prediction.

6. It is recommended to clarify the changes along the altitude.

Fig. 7 shows the MLA change along the altitude. MLA increases slightly with altitude and then decreases (line 259).

7. In Chapter 3, during the evaluation of the global MLA, a comparison between the predicted MLA and upscaled MLA samples is shown in Figure 12. However, this aspect is not presented in the part of the global MLA evaluation in Chapter 2. It is recommended to add relevant discussion to ensure consistency.

Thank you for your kindness. We have described this aspect in section 2.3.2 Global MLA mapping (line 185).

> *The prediction performance of the random forest regressor was evaluated using a ten-fold cross-validation approach with upscaled MLA samples.*

Reference

Amiri, R., Weng, Q., Alimohammadi, A., and Alavipanah, S. K.: Spatial–temporal dynamics of land surface temperature in relation to fractional vegetation cover and land use/cover in the Tabriz urban area, Iran, Remote Sens. Environ., 113, 2606-2617, 2009.

Bailey, B. N. and Mahaffee, W. F.: Rapid measurement of the three-dimensional distribution of leaf orientation and the leaf angle probability density function using terrestrial LiDAR scanning, Remote Sens. Environ., 194, 63-76, 10.1016/j.rse.2017.03.011, 2017.

Bayat, B., van der Tol, C., and Verhoef, W.: Integrating satellite optical and thermal infrared observations for improving daily ecosystem functioning estimations during a drought episode, Remote Sens. Environ., 209, 375-394, 10.1016/j.rse.2018.02.027, 2018.

Boonman, C. C. F., Benitez-Lopez, A., Schipper, A. M., Thuiller, W., Anand, M., Cerabolini, B. E. L., Cornelissen, J. H. C., Gonzalez-Melo, A., Hattingh, W. N., Higuchi, P., Laughlin, D. C., Onipchenko, V. G., Penuelas, J., Poorter, L., Soudzilovskaia, N. A., Huijbregts, M. A. J., and Santini, L.: Assessing the reliability of predicted plant trait distributions at the global scale, Glob Ecol Biogeogr, 29, 1034-1051, 10.1111/geb.13086, 2020.

Carlson, T. N. and Ripley, D. A.: On the relation between NDVI, fractional vegetation cover, and leaf area index, Remote Sens. Environ., 62, 241-252, https://doi.org/10.1016/S0034-4257(97)00104-1, 1997.

Carlson, T. N., Gillies, R. R., and Perry, E. M.: A method to make use of thermal infrared temperature and NDVI measurements to infer surface soil water content and fractional vegetation cover, Remote sensing reviews, 9, 161-173, 1994.

Chianucci, F., Pisek, J., Raabe, K., Marchino, L., Ferrara, C., and Corona, P.: A dataset of leaf inclination angles for temperate and boreal broadleaf woody species, Annals of Forest Science, 75, 50-50, 10.1007/s13595-018-0730-x, 2018.

Cui, L., Jiao, Z., Dong, Y., Sun, M., Zhang, X., Yin, S., Ding, A., Chang, Y., Guo, J., and Xie, R.: Estimating Forest Canopy Height Using MODIS BRDF Data Emphasizing Typical-Angle Reflectances, Remote Sensing, 11, 2239, 2019.

de Wit, C. T.: Photosynthesis of leaf canopies, Pudoc, 1965.

Dong, T., Liu, J., Shang, J., Qian, B., Ma, B., Kovacs, J. M., Walters, D., Jiao, X., Geng, X., and Shi, Y.: Assessment of red-edge vegetation indices for crop leaf area index estimation, Remote Sens. Environ., 222, 133-143, 10.1016/j.rse.2018.12.032, 2019.

Fang, H.: Canopy clumping index (CI): A review of methods, characteristics, and applications, Agricultural and Forest Meteorology, 303, 108374, https://doi.org/10.1016/j.agrformet.2021.108374, 2021.

Fang, H., Baret, F., Plummer, S., and Schaepman-Strub, G.: An Overview of Global Leaf Area Index (LAI): Methods, Products, Validation, and Applications, Rev. Geophys., 57, 739-799, 10.1029/2018rg000608, 2019.

Fang, H., Wang, Y., Zhang, Y., and Li, S.: Long-Term Variation of Global GEOV2 and MODIS Leaf Area Index (LAI) and Their Uncertainties: An Insight into the Product Stabilities, Journal of Remote Sensing, 2021, 1-17, 10.34133/2021/9842830, 2021.

Gitelson, A. A., Gritz †, Y., and Merzlyak, M. N.: Relationships between leaf chlorophyll content and spectral reflectance and algorithms for non-destructive chlorophyll assessment in higher plant leaves, J. Plant Physiol., 160, 271-282, https://doi.org/10.1078/0176-1617-00887, 2003.

Goel, N. S. and Thompson, R. L.: Inversion of vegetation canopy reflectance models for estimating agronomic variables. V. Estimation of leaf area index and average leaf angle using measured canopy reflectances, Remote Sens. Environ., 16, 69-85, 10.1016/0034-4257(84)90028-2, 1984.

Haboudane, D., Miller, J. R., Tremblay, N., Zarco-Tejada, P. J., and Dextraze, L.: Integrated narrow-band vegetation indices for prediction of crop chlorophyll content for application to precision agriculture, Remote Sens. Environ., 81, 416-426, https://doi.org/10.1016/S0034-4257(02)00018-4, 2002.

Iio, A., Hikosaka, K., Anten, N. P., Nakagawa, Y., and Ito, A.: Global dependence of field-observed leaf area index in woody species on climate: a systematic review, Global Ecol. Biogeogr., 23, 274-285, 2014.

Itakura, K. and Hosoi, F.: Estimation of Leaf Inclination Angle in Three-Dimensional Plant Images Obtained from Lidar, Remote Sensing, 11, 10.3390/rs11030344, 2019.

Jacquemoud, S., Flasse, S., Verdebout, J., and Schmuck, G.: Comparison of Several Optimization Methods To Extract Canopy Biophysical Parameters - Application To Caesar Data, 291-298, 1994.

Jacquemoud, S., Verhoef, W., Baret, F., Bacour, C., Zarco-Tejada, P. J., Asner, G. P., François, C., and Ustin, S. L.: PROSPECT+SAIL models: A review of use for vegetation characterization, Remote Sens. Environ., 113, S56-S66, 10.1016/j.rse.2008.01.026, 2009.

Jia, K., Liang, S., Liu, S., Li, Y., Xiao, Z., Yao, Y., Jiang, B., Zhao, X., Wang, X., Xu, S., and Cui, J.: Global Land Surface Fractional Vegetation Cover Estimation Using General Regression Neural Networks From MODIS Surface Reflectance, IEEE Transactions on Geoscience and Remote Sensing, 53, 4787-4796, 10.1109/tgrs.2015.2409563, 2015.

King, D. A.: The Functional Significance of Leaf Angle in Eucalyptus, Aust. J. Bot., 45, 619-639, https://doi.org/10.1071/BT96063, 1997.

Lang, R. H. and Saleh, H. A.: Microwave Inversion of Leaf Area and Inclination Angle Distributions from Backscattered Data, IEEE Transactions on Geoscience and Remote Sensing, GE-23, 685-694, 10.1109/TGRS.1985.289387, 1985.

Li, S., Fang, H., and Zhang, Y.: Determination of the Leaf Inclination Angle (LIA) through Field and Remote Sensing Methods: Current Status and Future Prospects, Remote Sensing, 15, 946, 2023.

Liu, J., Pattey, E., and Jégo, G.: Assessment of vegetation indices for regional crop green LAI estimation from Landsat images over multiple growing seasons, Remote Sens. Environ., 123, 347-358, 10.1016/j.rse.2012.04.002, 2012.

Moreno-Martínez, Á., Camps-Valls, G., Kattge, J., Robinson, N., Reichstein, M., van Bodegom, P., Kramer, K., Cornelissen, J. H. C., Reich, P., Bahn, M., Niinemets, Ü., Peñuelas, J., Craine, J. M., Cerabolini, B. E. L., Minden, V., Laughlin, D. C., Sack, L., Allred, B., Baraloto, C., Byun, C., Soudzilovskaia, N. A., and Running, S. W.: A methodology to derive global maps of leaf traits using remote sensing and climate data, Remote Sens. Environ., 218, 69-88, 10.1016/j.rse.2018.09.006, 2018.

Nilson, T.: A theoretical analysis of the frequency of gaps in plant stands, Agricultural meteorology, 8, 25-38, 1971.

Pisek, J., Ryu, Y., and Alikas, K.: Estimating leaf inclination and G-function from leveled digital camera photography in broadleaf canopies, Trees, 25, 919-924, 10.1007/s00468-011-0566-6, 2011.

Prentice, I. C., Balzarolo, M., Bloomfield, K. J., Chen, J. M., Dechant, B., Ghent, D., Janssens, I. A., Luo, X., Morfopoulos, C., Ryu, Y., Vicca, S., and van Hoolst, R.: Principles for satellite monitoring of vegetation carbon uptake, Nature Reviews Earth & Environment, 5, 818-832, 10.1038/s43017-024-00601-6, 2024.

Ryu, Y., Sonnentag, O., Nilson, T., Vargas, R., Kobayashi, H., Wenk, R., and Baldocchi, D. D.: How to quantify tree leaf area index in an open savanna ecosystem: A multi-instrument and multi-model approach, Agricultural and Forest Meteorology, 150, 63-76, 10.1016/j.agrformet.2009.08.007, 2010.

Schaaf, C. B., Gao, F., Strahler, A. H., Lucht, W., Li, X., Tsang, T., Strugnell, N. C., Zhang, X., Jin, Y., Muller, J.-P., Lewis, P., Barnsley, M., Hobson, P., Disney, M., Roberts, G., Dunderdale, M., Doll, C., d'Entremont, R. P., Hu, B., Liang, S., Privette, J. L., and Roy, D.: First operational BRDF, albedo nadir reflectance products from MODIS, Remote Sens. Environ., 83, 135-148, https://doi.org/10.1016/S0034-4257(02)00091-3, 2002.

Sulla-Menashe, D., Gray, J. M., Abercrombie, S. P., and Friedl, M. A.: Hierarchical mapping of annual global land cover 2001 to present: The MODIS Collection 6 Land Cover product, Remote Sens. Environ., 222, 183-194, 10.1016/j.rse.2018.12.013, 2019.

Svetnik, V., Liaw, A., Tong, C., Culberson, J. C., Sheridan, R. P., and Feuston, B. P.: Random forest: a classification and regression tool for compound classification and QSAR modeling, Journal of chemical information and computer sciences, 43, 1947-1958, 2003.

van Zanten, M., Pons, T. L., Janssen, J. A. M., Voesenek, L. A. C. J., and Peeters, A. J. M.: On the Relevance and Control of Leaf Angle, Crit. Rev. Plant Sci., 29, 300-316, 10.1080/07352689.2010.502086, 2010.

Wang, Q. and Ni-Meister, W.: Forest canopy height and gaps using BRDF index assessed with airborne lidar data, Remote Sensing, 11, 2566, 2019.

Wang, Q., Adiku, S., Tenhunen, J., and Granier, A.: On the relationship of NDVI with leaf area index in a deciduous forest site, Remote Sens. Environ., 94, 244-255, 2005.

Wang, Z., Schaaf, C. B., Lewis, P., Knyazikhin, Y., Schull, M. A., Strahler, A. H., Yao, T., Myneni, R. B., Chopping, M. J., and Blair, B. J.: Retrieval of canopy height using moderate-resolution imaging spectroradiometer (MODIS) data, Remote Sens. Environ., 115, 1595-1601, 2011.

Wei, S., Fang, H., Schaaf, C. B., He, L., and Chen, J. M.: Global 500 m clumping index product derived from MODIS BRDF data (2001–2017), Remote Sens. Environ., 232, 111296, https://doi.org/10.1016/j.rse.2019.111296, 2019.

Wu, C., Niu, Z., Tang, Q., and Huang, W.: Estimating chlorophyll content from hyperspectral vegetation indices: Modeling and validation, Agricultural and Forest Meteorology, 148, 1230-1241, https://doi.org/10.1016/j.agrformet.2008.03.005, 2008.

Yan, G., Jiang, H., Luo, J., Mu, X., Li, F., Qi, J., Hu, R., Xie, D., and Zhou, G.: Quantitative Evaluation of Leaf Inclination Angle Distribution on Leaf Area Index Retrieval of Coniferous Canopies, Journal of Remote Sensing, 2021, 1-15, 10.34133/2021/2708904, 2021.

Yan, K., Gao, S., Chi, H., Qi, J., Song, W., Tong, Y., Mu, X., and Yan, G.: Evaluation of the Vegetation-Index-Based Dimidiate Pixel Model for Fractional Vegetation Cover Estimation, IEEE Transactions on Geoscience and Remote Sensing, 60, 1-14, 10.1109/tgrs.2020.3048493, 2022.

Yang, X., Baskin, C. C., Baskin, J. M., Pakeman, R. J., Huang, Z., Gao, R., and Cornelissen, J. H. C.: Global patterns of potential future plant diversity hidden in soil seed banks, Nat Commun, 12, 7023, 10.1038/s41467-021-27379-1, 2021.

Zhang, P., Anderson, B., Barlow, M., Tan, B., and Myneni, R. B.: Climate - related vegetation characteristics derived from Moderate Resolution Imaging Spectroradiometer (MODIS) leaf area index and normalized difference vegetation index, Journal of Geophysical Research: Atmospheres, 109, 2004.

Zhang, Y.-W., Guo, Y., Tang, Z., Feng, Y., Zhu, X., Xu, W., Bai, Y., Zhou, G., Xie, Z., and Fang, J.: Patterns of nitrogen and phosphorus pools in terrestrial ecosystems in China, Earth System Science Data, 13, 5337-5351, 10.5194/essd-13-5337-2021, 2021.

Zheng, G. and Moskal, L. M.: Leaf orientation retrieval from terrestrial laser scanning (TLS) data, IEEE Transactions on Geoscience and Remote Sensing, 50, 3970-3979, 10.1109/TGRS.2012.2188533, 2012.

Zou, X. and Mõttus, M.: Retrieving crop leaf tilt angle from imaging spectroscopy data, Agricultural and Forest Meteorology, 205, 73-82, 10.1016/j.agrformet.2015.02.016, 2015.

Zou, X., Mõttus, M., Tammeorg, P., Torres, C. L., Takala, T., Pisek, J., Mäkelä, P., Stoddard, F. L., and Pellikka, P.: Photographic measurement of leaf angles in field crops, Agricultural and Forest Meteorology, 184, 137-146, 10.1016/j.agrformet.2013.09.010, 2014.